

Mass transfer limitations of mercury-biotransformation in multiphase reactor

S. Ledakowicz^{1,a,*}, U. Becker^b, W.-D. Deckwer^b

^a Technical University of Lodz, Department of Bioprocess Engineering, 90-924 Lodz, Poland

^b Gesellschaft für Biotechnologische Forschung mbH, 38124 Braunschweig, Germany

Abstract

A three-phase fluidized reactor with biocatalyst particles (immobilized bacteria *Pseudomonas putida* on polyvinyl alcohol matrix) has been employed for mercury removal from aqueous solution. The effective diffusivity D_{eff} of HgCl_2 in PVA hydrogel biocatalyst particle and the volumetric mass transfer coefficients for liquid–solid film $k_s a_s$ as well as for gas–liquid film $k_L a_L$ have been determined. Transport resistance evaluation revealed that in spite of significant intraparticle diffusion limitation (effectiveness factor in the range of 0.01), the both resistances of mass transfer around the catalyst particle and inside the catalyst pores should be taken into account.

1. Introduction

Mercury and its inorganic as well as organic compounds belong to the most toxic xenobiotica in our environment. Though the use of mercury compounds has been essentially reduced there are still many environmental risks and hazards as a result of its past industrial applications, e.g. the alkaline chlorine or acetaldehyde production.

For example, the German river Elbe and its banks are the most polluted areas upstream Hamburg (≤ 35 mg/kg soil) and therefore the average Hg contamination is about a factor of 100 higher than the natural background for this area. The limiting values for industrial waste water are fixed to be below 50 $\mu\text{g/l}$ and for drinking water below 1 $\mu\text{g/l}$.

Mercury as well as other heavy metals cannot be degraded by microorganisms, but can only be transformed from one oxidation state or organic complex to another; they accumulate in the environment and via the food chain in humans.

It was recently found at GBF, the German National Research Centre for Biotechnology in Braunschweig, that natural mercury resistant bacteria are able to effectively retain low concentrations of mercury present in a feed stream [1,2]. The mechanism of retention involves a reduction of the Hg^{II} to inert, volatile elemental Hg^0 , which relies on the activity of a cytosolic mercuric reductase.

Improved biocatalysts for mercury remediation were generated in GBF, by random mutagenesis of *Pseudomonas putida* with a minitransposon containing mer TPAB operon [3]. The mer T and mer P gene products are involved in Hg^{II} uptake and transport, mer A specifies the mercuric reductase and mer B encodes the organomercurial lyase.

* Corresponding author.

¹ Present address: TU Bergakademie Freiberg, Institut für Technische Chemie, 09599 Freiberg, Germany.

The ability to reduce Hg^{II} at increased rates in higher concentrations of mercurials was genetically combined with a benzene degradative pathway in order to prevent benzene release into the environment from phenylmercury splitting prior to reduction of Hg^{II} .

The genetically engineered microorganisms (GEM) of *P. putida* belong to in the lowest risk class (no harm for men, animals and environment). The GEMs were directly employed in fixed bed reactors after their immobilization on porous carriers (silica and alumina). However, this type of reactor configuration has many drawbacks: e.g. there are problems with the regeneration of the fixed bed and recovery of mercury accumulated in the bed, after 2–3 months of continuous work the fixed bed was clogged.

In order to overcome these disadvantages a new concept of the system has been proposed. Instead of two-phase flow fixed-bed a three-phase fluidized bed reactor has been employed. Introducing a gas flow which fluidizes beads of the biocatalyst, will additionally cause mercury volatilization and removal from the reactor.

Outside the multiphase reactor the mercury vapors may be condensed, sorbed or chemically bound and the gas should be recycled.

The present studies were aimed at the determination of mass transfer rates of individual steps and the evaluation of rate determining step.

2. Experimental

Fig. 1 shows the experimental set-up. It consists of:

- 1.5 l bubble column reactor (Bioengineering AG, Switzerland) equipped with pH, temperature and gas flow controlling units (not shown in the figure). A sampling device and necessary connections to inlet and outlet sections were additionally installed;
- absorption systems for outlet gas, containing Hg vapors, i.e. a gas washing bottle containing a oxidizing solution of KMnO_4 and H_2SO_4 , thermostated at 50°C (connected to the reflux condenser). An active carbon adsorber was additionally installed;
- analytical section (Atomic Absorption Spectrometer Perkin-Elmer M 2100 with cool vapor and hydride-generation techniques).

Before the bacteria were employed to mercury biotransformation in the fluidized bed reactor they had been first immobilized in a suitable matrix.

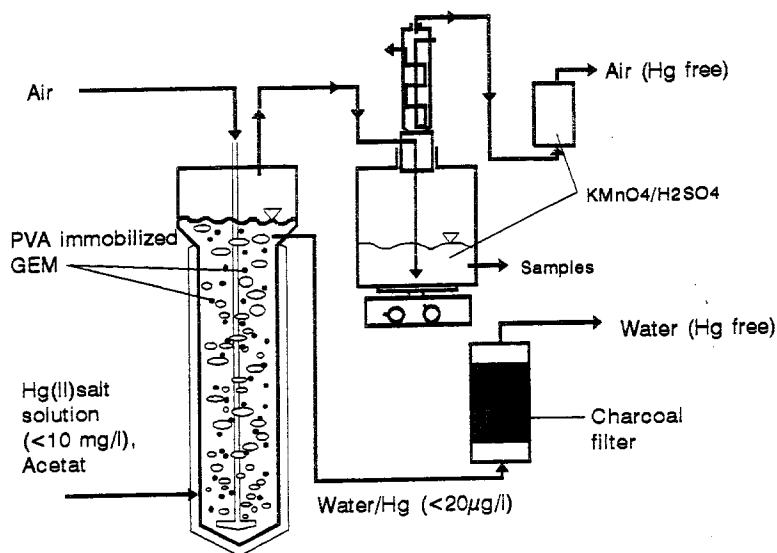


Fig. 1. Experimental set-up.

Polyvinyl alcohol (PVA) hydrogel has been chosen as the best suitable carrier. The entrapment method developed by Vorlop [4] is based on the gelation of an aqueous PVA solution which was frozen in liquid nitrogen.

The cryogel obtained from the GEMs suspension in PVA solution (10 wt.-%) with a high saponification rate and a polymerization degree (> 1500) had good stability and elasticity.

The immobilized GEMs *P. putida* KT2442::mer-73, in the form of gel-beads with an average diameter of 2.8 mm were introduced into the fluidized bed reactor and few experimental runs with active or inactive catalysts were carried out. The liquid concentrations of Hg^{II} and Hg^0 during batch experiments were followed by means of AAS technique.

3. Results and discussion

Before the cationic form of mercury Hg^{II} can react at the biocatalyst active centres, transport resistances must be overcome as shown in Fig. 2. The concentration pattern for the biotransformation product-elemental mercury Hg^0 is also present in the Fig. 2.

The following possible restrictions may arise:

- liquid–solid mass transfer of Hg^{II} -ions to the external catalyst surface, represented by $k_s a_s$ -volumetric mass transfer coefficient;
- simultaneous pore diffusion and biochemical reaction, represented by $k\eta$ — the product of pseudo-first order reaction constant (in the case of Michaelis-Menten kinetics $k = V_{\text{max}}/K_M$) and the catalyst effectiveness factor η ;
- effective diffusion of elemental Hg^0 inside the porous hydrogel, not considered in this study;
- solid–liquid mass transfer of Hg^0 from the external surface of the biocatalyst into liquid bulk, not considered in this study;
- liquid–gas mass transfer of metallic Hg^0 from the liquid into the gas phase \equiv desorption of mercury vapors, represented by the volumetric mass transfer coefficient $k_L a_L$.

At first, the study was concentrated on the determination of effective diffusivity of HgCl_2 in PVA hydrogel beads containing the immobilized bacteria. The instationary method of diffusivity determination according to Crank [5] allowed to estimate the effective diffusion coefficient D_{eff} . The calculation procedure and correlation of estimated D_{eff} with the biomass concentration in the PVA matrix will be published elsewhere [6].

Fig. 3 shows the original concentration data of HgCl_2 vs. time in the batch adsorption experiments in the bubble column with gel beads (1 part of inactive biomass and 20 parts of PVA) fluidized by an air superficial velocity of $u_G = 2.5$ cm/s.

In order to avoid Hg^{II} biotransformation during diffusion determination, the microorganisms were inactivated by streptomycin-sulfate. The values of effective pore diffusivity determined in the bubble column experiments were independent of superficial gas velocity and almost the same as D_{eff} determined in the stirred cell reactor [6].

It was possible to determine the external mass transfer $k_s a_s$ from the same curve of Hg^{II} concentration vs. time (Fig. 3). If one assumes that at the beginning ($t=0$) the surface concentration c^* is

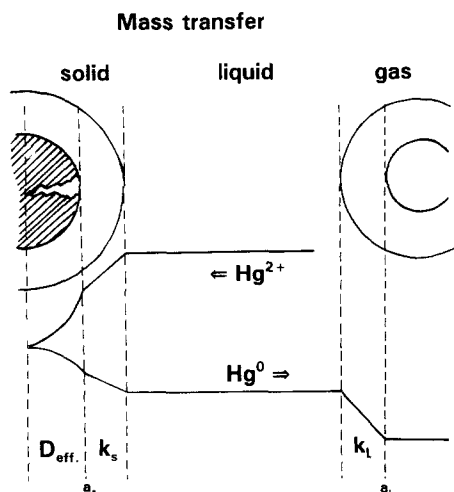


Fig. 2. Schematic representation of concentration pattern for substrate Hg^{II} and product Hg^0 .

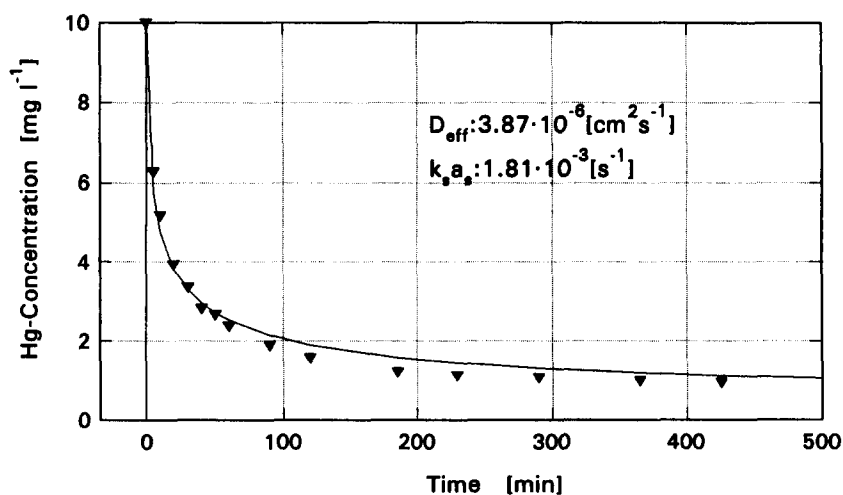


Fig. 3. Comparison of experimental (points) and theoretical results (solid line) for HgCl_2 diffusion from aqueous solution into an inactive biocatalyst.

negligible ($c^* = 0$) and as a consequence intra-particle diffusion is also negligible, the change in solute concentration $c(t)$ with respect to time t is:

$$-\frac{dc(t)}{dt} = k_s a_s (c(0) - 0) \quad (1)$$

then

$$-\frac{d \frac{c(t)}{c(0)}}{dt} \bigg|_{t=0} = k_s a_s \quad (2)$$

Hence, the initial slope of a plot $c(t)/c(0)$ vs. time enables $k_s a_s$ to be found.

Fig. 4 presents the $k_s a_s$ values vs. superficial gas velocity, together with the calculated asymptotic value of $k_s a_s$ (mass transfer from a static sphere into stagnant infinite fluid ($Sh = 2$)).

As it can be seen, $k_s a_s$ are independent of the gas flow rate above 1 cm/s. In order to determine the gas–liquid mass transfer coefficient $k_L a_L$ for desorption of the product Hg^0 , water saturated with Hg^0 was stripped with different gas flow rates.

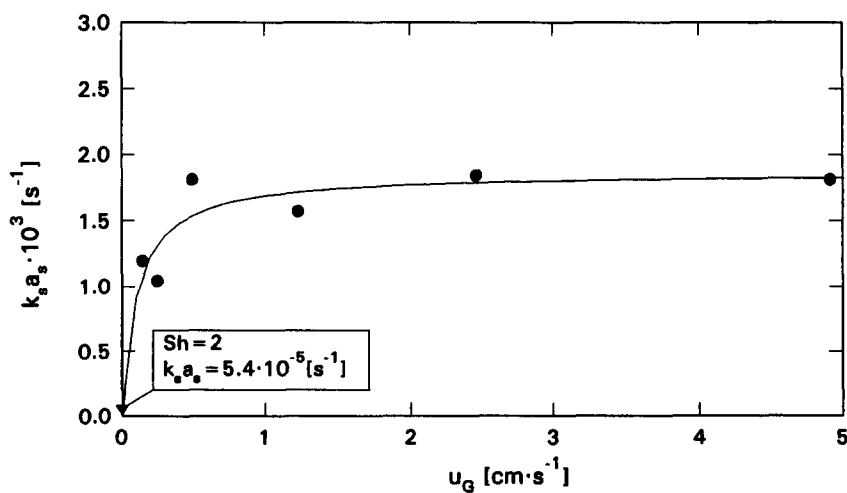


Fig. 4. Effect of gas velocity on volumetric solid–liquid mass transfer coefficient.

Fig. 5 shows the change in Hg^0 concentration in the liquid phase with respect to time for different gas flow rates.

The simplified model used to calculate the gas–liquid film mass transfer coefficient $k_L a_L$ for desorption of the product (metallic mercury)

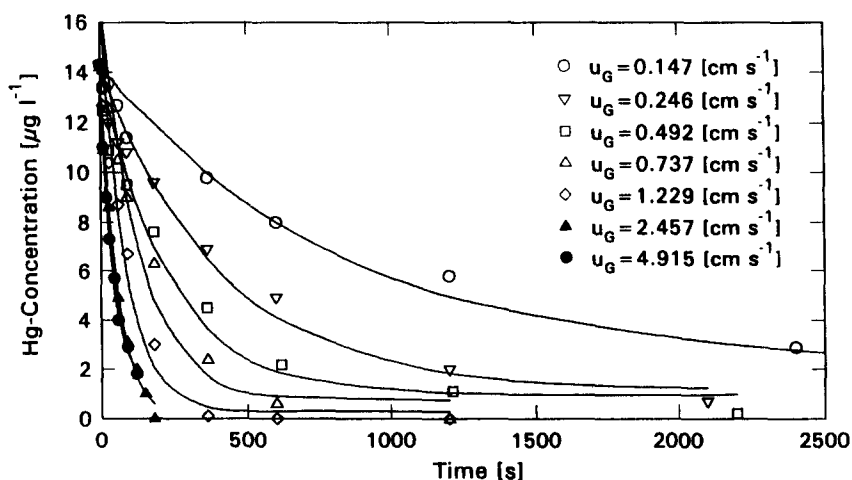


Fig. 5. Effect of varying gas velocity on Hg^0 concentration decay curves during batch desorption studies.

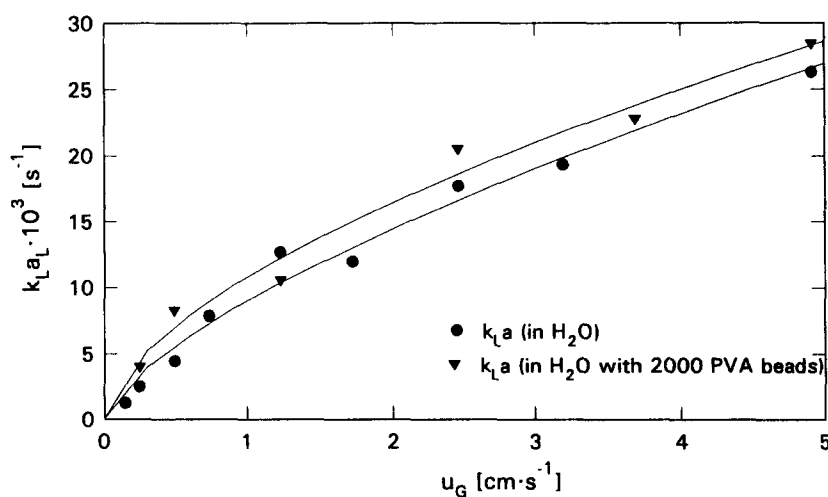


Fig. 6. Dependence of the $k_L a_L$ -values on gas velocity.

Table 1
Comparison of mass transfer limitations in a bubble column reactor

Superficial velocity of gas u_G (cm s^{-1})	$k_s a_s$ (s^{-1})	$1/k_s a_s$ (s^1)	D_{eff} ($\text{cm}^2 \text{s}^{-1}$)	$t_D = d^2/D_{\text{eff}}$ (s^1) ($d=0.28 \text{ cm}$)	$k_L a_L$ (s^{-1})	$1/k_L a_L$ (s^1)
0.2457	$1.04 \cdot 10^{-3}$	$9.62 \cdot 10^2$	$3.87 \cdot 10^{-6}$	$2.026 \cdot 10^4$	$2.5 \cdot 10^{-3}$	$4.00 \cdot 10^2$
0.4915	$1.81 \cdot 10^{-3}$	$5.53 \cdot 10^2$	$4.05 \cdot 10^{-6}$	$1.936 \cdot 10^4$	$4.5 \cdot 10^{-3}$	$2.22 \cdot 10^2$
1.2287	$1.57 \cdot 10^{-3}$	$6.37 \cdot 10^2$	$3.97 \cdot 10^{-6}$	$1.975 \cdot 10^4$	$12.7 \cdot 10^{-3}$	$0.78 \cdot 10^2$
2.4574	$1.84 \cdot 10^{-3}$	$5.44 \cdot 10^2$	$3.87 \cdot 10^{-6}$	$2.026 \cdot 10^4$	$17.7 \cdot 10^{-3}$	$0.57 \cdot 10^2$
4.9147	$1.81 \cdot 10^{-3}$	$5.53 \cdot 10^2$	$4.28 \cdot 10^{-6}$	$1.832 \cdot 10^4$	$26.3 \cdot 10^{-3}$	$0.38 \cdot 10^2$

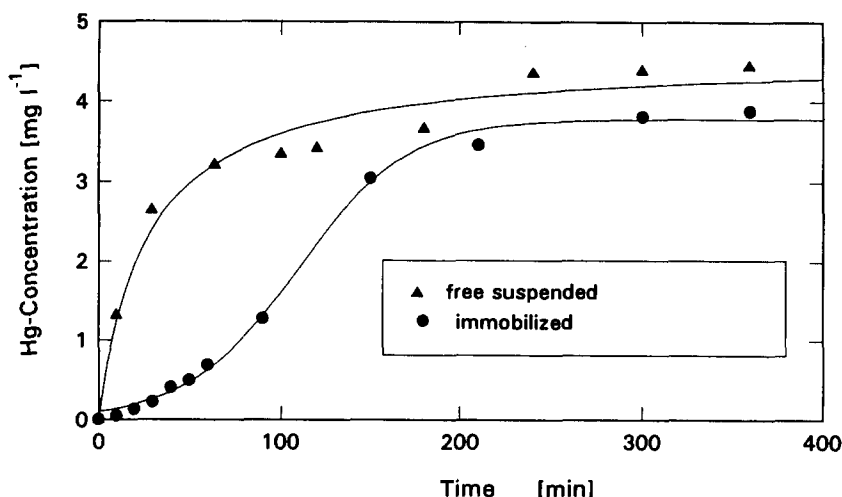


Fig. 7. Kinetic curves for freely suspended and immobilized bacteria *P. putida* KT2442::mer-73.

from an aqueous solution assumed that the batch liquid phase is perfectly mixed with gas bubbles.

The governing mass balance equation is

$$-\frac{dc_L}{dt} = k_L a_L (c_L - c_L^*) \quad (3)$$

where $c_L^* = p/He$ is the concentration of Hg^0 at the gas–liquid interface.

Separate experiments were performed to determine Henry's constant He for the system mercury/water. The value of Henry's constant for the system under the experimental conditions was determined as $He = 0.8$ (Pa·dm³/mol). More details may be found elsewhere [7].

Integration of the mass balance equation with the initial conditions $t = 0$, $c_L = c_L^0$ gives

$$c_L(t) = c_L^* + (c_L^0 - c_L^*) \exp(-k_L a_L t) \quad (4)$$

The decay curves fitting (solid lines in Fig. 5) enables to calculate $k_L a_L$ -values with the Marquardt–Levenberg algorithm.

The dependence of the $k_L a_L$ -values on gas velocity is presented in Fig. 6 with and without inert catalyst beads.

In contrary to liquid–solid mass transfer coefficient $k_s a_s$, the gas–liquid mass transfer coefficient $k_L a_L$, as expected, depends strongly on the gas flow rate. The presence of solid particle increases, to rather small extent, the $k_L a_L$ -values. The influence of superficial gas velocity on mass transfer

coefficients were summarized in Table 1. The reciprocals of mass transfer coefficient as the measure of mass transfer resistance are also shown in Table 1.

However, the most important is the chemical reaction, i.e. mass transfer interaction for the mercury biotransformation. In order to evaluate the so-called reaction time, one needs the intrinsic kinetic parameters of Michaelis–Menten equation. They were separately determined for freely suspended (not immobilized) bacteria *P. putida*:

$$V_{\max} = 2 \mu\text{mol dm}^{-3} \text{ s}^{-1} \text{ and } K_M = 4 \mu\text{mol dm}^{-3}.$$

The constant for pseudo first order reaction estimated for our case was $k = V_{\max}/K_M = 0.5 \text{ s}^{-1}$.

Comparison of effective diffusion time with reaction time ($t_R = 1/k$) gives Thiele modulus $\Phi = (t_D/t_R)^{1/2} = 100$. Such a large value of Φ indicates a high level of pore diffusion limitation. Therefore, the effectiveness factor $\eta = 1/\Phi$ is expected to be in the range of 10^{-2} . The estimated effectiveness factor may be compared with the experimental/apparent value calculated from the data presented in Fig. 7.

Fig. 7 shows the comparison of kinetic curves (Hg^0 -concentrations in the gas phase versus time) for freely suspended bacteria and the same amount of biomass immobilized in PVA gel. The ratio of initial slopes of the curves (at $t \rightarrow 0$) gives the apparent effectiveness factor

$$\eta_{\text{exp}} = \left[\frac{(dc/dt)_{\text{immo}}}{(dc/dt)_{\text{free}}} \right]_{t=0} = 0.04 \quad (5)$$

which is in the fairly good agreement with the calculated value of $\eta = 0.01$.

In spite of significant intraparticle diffusion limitation, the biochemical reaction is so fast that the pore diffusion is not the rate determining step, because for large biocatalyst particles the external mass transfer resistance is even greater than the internal diffusion resistance.

This conclusion followed from the comparison of relative resistances of mass transfer and chemical reaction

$$1/k_s a_s = 1000 \text{ s} > 1/k\eta = 200 \text{ s} \quad (6)$$

as well as from global effectiveness factor η_G which includes both resistances

$$1/\eta_G = 1/\eta + \Phi^2/Sh \approx 100 + 136 \quad (7)$$

where $Sh = k_s r / D_{\text{eff}} = 73.5$ ($r = 0.14$ cm average catalyst radius) is the modified Sherwood number.

The future work will be carried out with smaller catalyst particles and new type of immobilized catalyst (shell biocatalyst).

Acknowledgements

S. Ledakowicz thanks the Commission of the European Community for the Mobility Fellowship ERB-CIPA-CT 92-0047.

References

- [1] A. Frischmuth, Ph.D. Thesis TU Braunschweig, 1991.
- [2] M. Röhrich, Mikrobielle Verfahren zur Entfernung von Schwermetallen aus wäßrigen Lösungen, VDI Fortschritt Berichte Reihe 15, Nr. 101, VDI-Verlag, Düsseldorf, 1993.
- [3] J.M. Horn, M. Brunke, W.-D. Deckwer and K.N. Timmis, Appl. Environ. Microbiol., 60 (1994) 357.
- [4] K.D. Vorlop and P. Remmers, Ger. Pat. DE 4027218 (1991).
- [5] J. Crank, The Mathematics of Diffusion, Clarendon Press, Oxford, 1975.
- [6] U. Becker, W.-D. Deckwer and S. Ledakowicz, Biotechnol. Bioeng. (1995) in preparation.
- [7] S. Ledakowicz, U. Becker and W.-D. Deckwer, Chem. Eng. Sci. (1995) in preparation